A&A 431, 673–677 (2005)
DOI: 10.1051/0004-6361:20041790

Astronomy & Astrophysics

Research Note

An upper bound on the energy of a gravitationally redshifted electron-positron annihilation line from the Crab pulsar

P. S. Negi

Department of Physics, Kumaun University, Nainital - 263 002, India
e-mail: negi@upso.ernet.in

Received 4 August 2004 / Accepted 5 November 2004

Abstract. We present a causally consistent and pulsationally stable two component neutron star model on the basis of the criterion that for each assigned value of $\sigma(\equiv(P_0/E_0) \equiv$ the ratio of central pressure to central energy-density), the compactness ratio $u(\equiv(M/R)$, where M is the total mass and R is the radius of the configuration) of the static configuration does not exceed the compactness ratio, $u_{\rm h}$, of the homogeneous density sphere (that is, $u \leq u_{\rm h}$). The core of this model is given by the stiffest equation of state (EOS), $\mathrm{d}P/\mathrm{d}E = 1$ (in geometrized units) and the envelope is characterized by the well-known EOS of a classical polytrope $\mathrm{d}\ln P/\mathrm{d}\ln\rho = \Gamma_1[(4/3) \leq \Gamma_1 \leq 2]$. The models yield an upper bound on surface redshift, $z_{\rm R} \simeq 0.77$, of neutron stars corresponding to the case of $\Gamma_1 = 5/3$ envelope, whereas a model-independent upper bound on neutron star masses, $M_{\rm max} \leq 4.1\ M_\odot$, is obtained for a conservative choice of the "matching density", $E_{\rm b} = 2.7 \times 10^{14}$ g cm^{-3}, at the core-envelope boundary. If the observational constraint of the glitch healing parameter, $Q \geq 0.7$, of the Crab pulsar is imposed on these models, the strong lower bounds on surface redshift $z_{\rm R} \geq 0.2234$ and mass $M \simeq 1.721\ M_\odot$ are obtained for the Crab pulsar. However, if the other observational constraint of the recently evaluated value of the moment of inertia for the Crab pulsar (based upon the newly estimated "central value" of the Crab nebula mass M(nebula) $\simeq 4.6\ M_\odot$) is also imposed on these models together with the observational constraint of the "central" weighted mean value $Q \approx 0.72$, the model with the $\Gamma_1 = 5/3$ envelope itself yields the value of matching density, $E_{\rm b} = 2.7 \times 10^{14}$ g cm^{-3}, adopted in this study and in this sense does not represent a fiduciary quantity. For these constraints, the minimum surface redshift and mass of the Crab pulsar are slightly increased to the values $z_{\rm R} \simeq 0.2350$ and $M \simeq 1.807\ M_\odot$ respectively. The confirmation of these results requires evidence of the observation of the gravitationally redshifted electron-positron annihilation line in the energy range of about 0.414–0.418 MeV from the Crab pulsar, which is in agreement with the energy of the gamma-ray line at about 0.40 MeV, observed in the mid 1970s.

Key words. dense matter – equation of state – stars: neutron – pulsars: individual: Crab

1. Introduction

The observational data on neutron star (NS) parameters place stringent constraints on the equations of state (EOSs) of dense nuclear matter. Among them, the data on the glitch healing parameter, Q, in particular, for the Crab and Vela pulsars are extensively and accurately known at present (see, e.g. Crawford & Demiański 2003, and references therein). Such data also provide the best tool for testing the starquake (Ruderman 1972; Alpar et al. 1996) and Vortex unpinning (Alpar et al. 1993) models of glitch mechanisms. In the starquake model, Q is defined as the fractional moment of inertia, i.e. the ratio of the moment of inertia of the superfluid core, $I_{\rm core}$, to the moment of inertia of the entire configuration, $I_{\rm total}$, as (Pines et al. 1974)

$$Q = \frac{I_{\rm core}}{I_{\rm total}}. \tag{1}$$

Recently, Crawford & Demiański (2003) have collected the all measured values of the glitch healing parameter Q for Crab and Vela pulsars available in the literature and found that for 21 measured values of Q for Crab glitches, a weighted mean of the values yields $Q = 0.72 \pm 0.05$, and the range of $Q \geq 0.7$ encompasses the observed distribution for the Crab pulsar. In order to test the starquake model for the Crab pulsar, they have computed Q (as given by Eq. (1)) values for seven representative EOSs of dense nuclear matter, covering a range of neutron star masses. Their study shows that the much larger values of $Q(\geq 0.7)$ for the Crab pulsar are fulfilled by all but the six EOSs considered in the study corresponding to a "realistic" neutron star mass range $1.4 \pm 0.2\ M_\odot$. Furthermore, the minimum value of NS mass, corresponding to the minimum value of $Q \simeq 0.7$ (in the range that encompasses the observed distribution for Crab pulsar) for the models is $\simeq 0.15\ M_\odot$.

Although the results of the study are consistent with the starquake model predictions, it appears that even such extensive and accurate data on the glitch healing parameter are unable to put any strong constraint on the EOSs of dense nuclear matter. Most of the NS models based upon such EOSs can easily satisfy the requirement of $Q(\geq 0.7)$ for the mass range $1.4 \pm 0.2\ M_\odot$. The reason for this is that in all conservative models of NSs, the choice of the core-envelope boundary, r_b (corresponding to a density denoted by E_b), is somewhat *arbitrary* in the sense that there are no criteria available for the choice of a particular matching density, E_b, below which the EOS of the NS matter is assumed to be known and unique. One can freely choose somewhat lower values of E_b (which will increase the core size) to obtain higher values of Q (see, e.g. Shapiro & Teukolsky 1983; Datta & Alpar 1993).

Recently, we have obtained a criterion (based upon the well-known principle that for a given M and R, the minimum central pressure corresponds to the sphere of homogeneous density distribution; see, e.g. Wienberg 1972) which asserts that for an assigned value σ, the compactness parameter u of any *regular* configuration should not exceed the compactness parameter u_h of the homogeneous density sphere, in order to assure the compatibility with the hydrostatic equilibrium (Negi & Durgapal 2001; Negi 2004a). This criterion is capable of constraining the core-envelope boundary of any physically realistic NS model. A combination of this criterion with those of the observational data on the glitch healing parameter and the recently estimated minimum value of the moment of inertia for the Crab pulsar (based upon the newly estimated "central value" of the Crab nebula mass $M(\mathrm{nebula}) \simeq 4.6\ M_\odot$), $I_{\mathrm{Crab},45} = 3.04$; where $I_{\mathrm{Crab},45} = I_\mathrm{Crab}/10^{45}\ \mathrm{g\,cm^2}$ (Bejger & Haensel 2002) can provide strong constraints on the EOSs of dense nuclear matter.

In the present paper, we adopt the abovementioned combination to construct NS models for the Crab pulsar by considering a core of most stiff material represented by $\mathrm{d}P/\mathrm{d}E = 1$ (where P is the pressure and E the energy-density) and the envelope is characterized by the well-known EOS of the classical polytrope $\mathrm{d}\ln P/\mathrm{d}\ln\rho = \Gamma_1$ (where ρ is the density of the rest-mass and Γ_1 is a constant known as the adiabatic index) for $\Gamma_1 = (4/3), (5/3)$ and 2 respectively. The EOS in the core is justified because the various observational studies (e.g. the gamma-ray burst data, X-ray burst data and the glitch data etc.) and their explanation (see, e.g. Lindblom 1984; Cottam et al. 2002; Datta & Alpar 1993) favour the stiffest EOSs. The latest estimate of the moment of inertia of the Crab pulsar (based upon the "newest" observational data on the Crab nebula mass) also supports the stiffest EOSs (Bejger & Haensel 2002). (This justification also follows from the fact that EOSs of the dense nuclear matter beyond the density range $\simeq 10^{14}\ \mathrm{g\,cm^{-3}}$ are not well known because of the lack of knowledge of nuclear interactions (see, e.g. Dolan 1992, and references therein), and the various EOSs available in the literature (see, e.g. Arnett & Bowers 1977) for NS matter represent only an extrapolation of the results far beyond this density range. Since the status of the "real" EOS for NS matter is not certain, one could impose some well-known physical principle, independent of the EOS, such as the "causality condition" ($\mathrm{d}P/\mathrm{d}E = 1$) throughout the core of the star beyond a fiduciary density at the core-envelope boundary (see, e.g. Rhoades & Ruffini 1974; Hartle 1978; Lindblom 1984; Friedman & Ipser 1987; Kalogera & Baym 1996). Such models are generally called "physically realistic"). The polytropic EOS with $\Gamma_1 = 4/3$ represents the EOS of extreme relativistic degenerate electrons and non-relativistic nuclei (Chandrasekhar 1935), $\Gamma_1 = (5/3)$ represents the well-known EOS of non-relativistic degenerate "neutron gas" (Oppenheimer & Volkoff 1939), and $\Gamma_1 = 2$ represents the case of extreme relativistic baryons interacting through a vector meson field (Zeldovich 1962). It follows, therefore, that the polytropic EOS for the said Γ_1 values can cover nearly the entire density range for NS matter which is also applicable for the envelope region and not may be even more convincing to use an average (constant) value of Γ_1 below the density range E_b, instead of the details of this density range specified by various EOSs like BPS (Baym et al. 1971), NV (Negele & Vautherin 1973), or FPS (Lorenz et al. 1993), which are frequently used by various authors in the conventional models of NSs (Friedman & Ipser 1987; Kalogera & Baym 1996) despite their uncertainty in the sense mentioned above. Such study can also provide insight into the appropriateness of the EOS for the envelope region, since both the theory (criterion) and the observations (stated above) are used to construct the NS models.

2. Methodology

The metric for spherically symmetric and static configurations can be written in the following form

$$\mathrm{d}s^2 = \mathrm{e}^{\nu}\mathrm{d}t^2 - \mathrm{e}^{\lambda}\mathrm{d}r^2 - r^2\mathrm{d}\theta^2 - r^2\sin^2\theta\mathrm{d}\phi^2, \tag{2}$$

where ν and λ are functions of r alone. The Oppenheimer-Volkoff (O-V) equations (Oppenheimer & Volkoff 1939), resulting from the Einstein field equations for systems with isotropic pressure P and energy-density E can be written as

$$P' = -(P+E)[4\pi Pr^3 + m]/r(r-2m) \tag{3}$$

$$\nu'/2 = -P'/(P+E) \tag{4}$$

$$m'(r) = 4\pi Er^2; \tag{5}$$

where the prime denotes the radial derivative and $m(r)$ represents the mass contained within the radius r

$$m(r) = \int_0^r 4\pi Er^2\mathrm{d}r.$$

The coupled Eqs. (3)–(5), are solved for the model (supplemented by the boundary conditions: $P = E = 0$, $m(r = R) = M$, $\mathrm{e}^{\nu} = \mathrm{e}^{-\lambda} = (1 - 2M/R) = (1 - 2u)$ at $r = R$) by considering the EOS, $\mathrm{d}P/\mathrm{d}E = 1$, in the core and choosing various values of Γ_1 in the polytropic envelope for various assigned values of σ such that for each value of σ, the compactness ratio of the whole configuration always turns out to be less than or equal to the compactness ratio of the corresponding sphere (with the same σ) of the homogeneous density distribution. We find that this condition is uniquely fulfilled by all models corresponding to an envelope with $\Gamma_1 = (4/3), (5/3)$

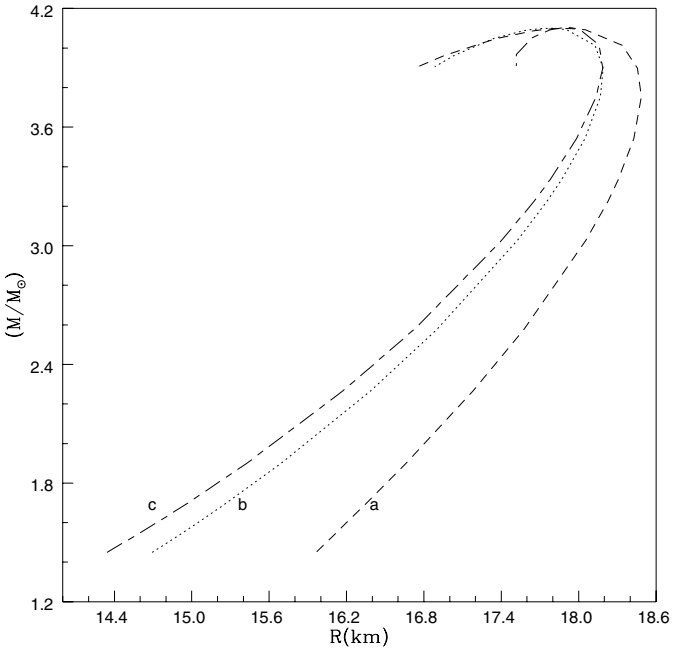

Fig. 1. Mass–radius diagram of the models as discussed in the text for an assigned value of matching density $E = E_b = 2.7 \times 10^{14}$ g cm^{-3} at the core-envelope boundary. The labels a, b and c represent the models for an envelope with $\Gamma_1 = (4/3), (5/3)$ and 2 respectively. The minimum value of the ratio of pressure to energy-density, (P_b/E_b), at the core envelope boundary is obtained as 1.065×10^{-2}, such that for an assigned value of σ, the inequality $u \leq u_h$ is always satisfied, as shown in Table 1.

and 2, if the *minimum* value of the ratio of pressure to energy-density, P_b/E_b, at the core-envelope boundary reaches about 1.065×10^{-2}. The results of the study are presented in Fig. 1 for a conservative choice of $E_b = 2.7 \times 10^{14}$ g cm^{-3}, the nuclear saturation density (note that the conservative choice of E_b used here turns out to be a consequence of the present study, and therefore, does not represent a fiduciary quantity as discussed in the next section). It is seen that the models become pulsationally stable up to the maximum value of mass $M_{max} \simeq 4.1\ M_\odot$ and radius, $R \simeq 17.81-17.94$ km. The minimum radius results for the model with a $\Gamma_1 = (5/3)$ envelope thus maximizes the compactness ratio for the stable configuration, $u \simeq 0.34$, as shown in Table 1 (this upper bound is found to be fully consistent with the *exact* absolute upper bound on compactness ratio of NSs compatible with causality and pulsationally stability, obtained elsewhere; see, e.g. Negi 2004b). This behaviour indicates the appropriateness of the model with the $\Gamma_1 = (5/3)$ envelope among various values of Γ_1 chosen in the envelope. The binding energy per unit mass $\alpha(\equiv(M_r - M)/M$; where M_r is the rest-mass (see, e.g. Shapiro & Teukolsky 1983)) also approaches a maximum for about 0.3235 for the maximum value of mass up to which the configurations remain pulsationally stable.

3. An application of the models to the Crab pulsar

For slowly rotating configurations like the Crab pulsar (rotation velocity about 188 rad s^{-1}) the moment of inertia may be

Table 1. Various values of compactness ratio corresponding to the configurations presented in Fig. 1 for different assigned values of σ. The compactness ratio for a homogeneous density distribution is represented by u_h. The slanted values correspond to the limiting case up to which the configuration remains pulsationally stable.

(P_0/E_0)	u_h	u_a	u_b	u_c
0.11310	0.15464	0.13441	0.14576	0.14920
0.11978	0.16070	0.14095	0.15210	0.15546
0.12544	0.16567	0.14633	0.15730	0.16060
0.13235	0.17152	0.15267	0.16344	0.16666
0.15071	0.18603	0.16843	0.17869	0.18171
0.18605	0.21029	0.19489	0.20427	0.20695
0.22013	0.23000	0.21649	0.22510	0.22748
0.28047	0.25823	0.24752	0.25498	0.25685
0.31322	0.27081	0.26132	0.26825	0.26987
0.33333	0.27778	0.26895	0.27558	0.27703
0.37791	0.29149	0.28387	0.28987	0.29099
0.43583	0.30640	0.29991	0.30517	0.30582
0.48898	0.31785	0.31192	0.31654	0.31673
0.55022	0.32898	0.32317	0.32707	0.32660
0.63427	0.34152	0.33476	0.33757	0.33586
0.66102	0.34498	*0.33761*	*0.34002*	*0.33777*
0.68401	0.34778	0.33972	0.34175	0.33896
0.70503	0.35021	0.34137	0.34301	0.33964
0.71465	0.35128	0.34205	0.34350	0.33982
0.75963	0.35600	0.34435	0.34474	0.33923
0.81199	0.36095	0.34504	0.34360	0.33449
0.83724	0.36314	0.34430	0.34156	0.32962

calculated in the first order approximation that appears in the form of the Lense-Thirring frame dragging-effect. For Crab and Vela pulsars, the first-order effects turn out to be about 1–2% (other effects like mass shift and deformation from spherical symmetry due to rotation represent second-order effects which are significant for the case of millisecond pulsars. For Crab and Vela like pulsars, the second-order effects turn out to be about 10^{-4} or even lower; see, e.g. Arnett & Bowers; Crawford & Demiański 2003. Therefore, these effects can be safely ignored when studying the macroscopic parameters of the slowly rotating pulsars as carried out in the present paper). These effects are reproduced by an empirical formula that is based on the numerical results obtained for thirty theoretical EOSs of dense nuclear matter. For NSs, the formula yields (Bejger & Haensel 2002)

$$I \simeq \frac{2}{9}(1 + 5x)MR^2, \quad x > 0.1 \tag{6}$$

where x is the compactness ratio measured in units of $(M_\odot(\mathrm{km})/\mathrm{km})$, i.e.

$$x = \frac{M/R}{M_\odot/\mathrm{km}} = \frac{u}{1.477} \tag{7}$$

only static (non-rotating) parameters of the spherical configuration appear in the formula.

Equation (6) is used, together with coupled Eqs. (3)–(5), to calculate the fractional moment of inertia given by Eq. (1) and

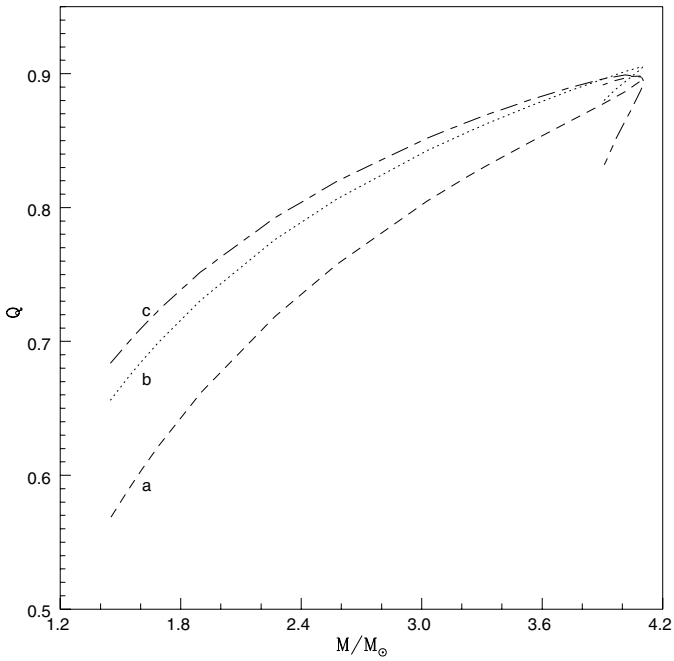

Fig. 2. Fractional moment of inertia $Q(\equiv I_{\rm core}/I_{\rm total})$ vs. total mass M for the configurations presented in Fig. 1. The labels a, b and c represent the models for an envelope with $\Gamma_1 = (4/3), (5/3)$ and 2 respectively.

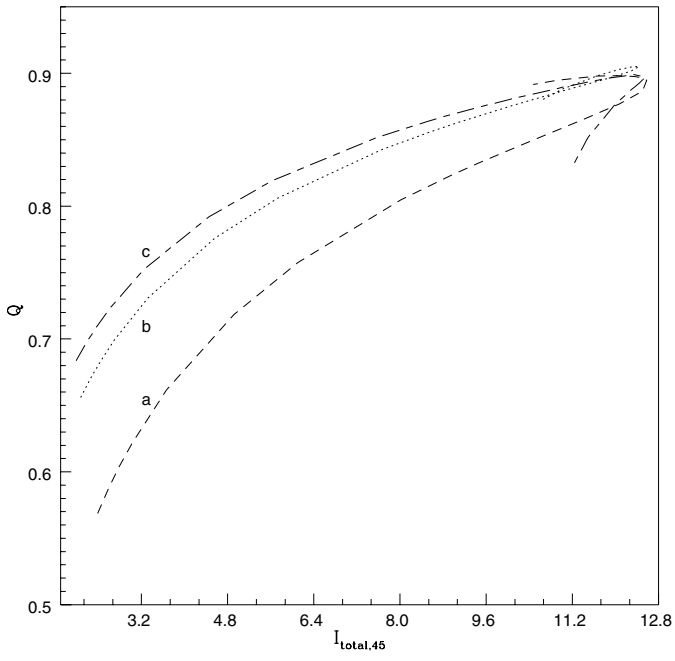

Fig. 3. Fractional moment of inertia $Q(\equiv I_{\rm core}/I_{\rm total})$ vs. moment of inertia of the whole structure $I_{\rm total,45}$ for the configurations presented in Fig. 1. The labels a, b and c represent the models for an envelope with $\Gamma_1 = (4/3), (5/3)$ and 2 respectively. $I_{\rm total,45}$ is defined as $I_{\rm total}/10^{45}\,{\rm g\,cm^2}$.

the moment of inertia of the entire configuration for configurations presented in Fig. 1. The results are shown in Figs. 2 and 3 respectively. For the minimum value of $Q \simeq 0.7$ (in the range that encompasses the observed distribution for the Crab pulsar), Fig. 2 yields the minimum masses $M \simeq 1.57\ M_\odot, 1.72\ M_\odot$, and $2.15\ M_\odot$ for the models with an envelope $\Gamma_1 = 2, (5/3)$, and (4/3) respectively. The corresponding values of surface redshift, $z_{\rm R}$, turn out to be 0.2101, 0.2234, and 0.2628 respectively. If the other observational constraint of $I_{\rm Crab,45} = 3.04$ is also imposed on these models together with $Q \geq 0.7$, the model with a $\Gamma_1 = (4/3)$ envelope is ruled out because it gives a minimum mass $M \simeq 1.696\ M_\odot$ for $Q \simeq 0.623$ as is evident from Fig. 3. For the last two constraints, the models with $\Gamma_1 = (5/3)$ and 2 yield the minimum masses $M \simeq 1.807\ M_\odot, 1.837\ M_\odot$ and the surface redshifts $z_{\rm R} \simeq 0.2350$, 0.2450 respectively. The corresponding Q values are obtained as $Q \simeq 0.718$ and 0.744 for $\Gamma_1 = (5/3)$ and 2 cases respectively (note that $Q(\text{for}\,\Gamma_1 = 5/3) < Q(\text{for}\,\Gamma_1 = 2)$, and represents approximately the "central" weighted mean value of $Q \simeq 0.72$. Thus, for the observational constraint of the "central" weighted mean value $Q \approx 0.72$, and $I_{\rm Crab,45} = 3.04$, the model with the $\Gamma_1 = (5/3)$ envelope itself yields the value of matching density, $E_{\rm b} = 2.7 \times 10^{14}$ g cm^{-3}, adopted in the present study). It follows, therefore, that both theoretical and observational studies support the NS model with an envelope given by a polytrope of index $n = 3/2$. The minimum value of surface redshift corresponding to this model in the range 0.2234–2350 would require an observation of the gravitationally redshifted radiation in the energy range of about 0.414–0.418 MeV, which agrees quite well with the observation of a gamma-ray line at about 0.40 MeV from the Crab pulsar (Leventhal et al. 1977). Note, however, that there is no evidence in favour of the claim of a 0.44 MeV annihilation line from the Crab pulsar by the FIGARO team (see, e.g. Ulmer et al. 2001; and references therein). Obviously, the lower bounds on surface redshift obtained here do not represent, in general, the absolute lower bound on surface redshift of NSs.

4. Implications of the models for the extraordinary gamma-ray burst GRB790305b

Apart from the models of the Crab pulsar, let us consider two of the main findings related to the extraordinary gamma-ray burst of 5 March 1979: (i) it gives the only reliable estimate of the surface redshift, $z_{\rm R} = 0.23 \pm 0.07$ (after taking due account of thermal blueshift), associated with the supernova remnant N49 in the Large Magellanic Cloud (see, e.g. Higdon & Lingenfelder 1990; Douchin & Haensel 2001, and references therein); and (ii) the implied peak luminosities of the repeating burst GRB 790305b correspond to an energy of 10^{44} erg, which is possible only when a starquake releases at least 10^{-9} of the NS gravitational binding-energy of 10^{53} erg (Higdon & Lingenfelder 1990). In order to reproduce both of these findings, one would require a NS model compatible with starquake model predictions (assuming $Q \geq 0.7$, as in the case of the Crab pulsar) that could also account for a surface redshift $z_{\rm R} = 0.23 \pm 0.07$. Both of these requirements are, in fact, fulfilled by our models. For the case of the $\Gamma_1 = 5/3$ envelope model, we get from Fig. 2–3 the central value of surface redshift $z_{\rm R} = 0.23$ for a mass $M \simeq 1.776\ M_\odot$ with $Q \simeq 0.713$. The binding energy corresponding to this case is obtained as 4.289×10^{53} erg which is capable of releasing 4.289×10^{44} erg of energy required for the latter burst.

5. Results and conclusions

This study shows that the stable sequences of NS models terminate at the value of maximum mass, $M_{\max} \simeq 4.1\ M_{\odot}$, independent of the EOSs of the envelope, for the matching density, $E_{\rm b} = 2.7 \times 10^{14}$ g cm^{-3}, at the core-envolope boundary. The "matching density" is a consequence of the study and in this sense does not represent a fiduciary quantity. The upper bound of the surface redshift, $z_{\rm R} \simeq 0.77$ (corresponding to a u value $\simeq$0.34), however, belongs to the model with a $\Gamma_1 = 5/3$ envelope which is consistent with the absolute upper bound on the surface redshift of NS models compatible with causality and pulsational stability (Negi 2004b).

For this appropriate NS model (with a $\Gamma_1 = 5/3$ envelope) a minimum surface redshift of the Crab pulsar is 0.223, if the observational constraint of the glitch healing parameter $Q \simeq 0.7$ is imposed. This value gives the minimum mass of the Crab pulsar $M \simeq 1.721\ M_{\odot}$ for the "matching density" $E_{\rm b} = 2.7 \times 10^{14}$ g cm^{-3} at the core-envelope boundary. The minimum surface redshift and mass are slightly increased up to the values $z_{\rm R} \simeq 0.235$ and $M \simeq 1.807\ M_{\odot}$ respectively, if the newly estimated "central" value of the moment of inertia $I_{\rm Crab,45} \simeq 3.04$, based on the recent estimate of the Crab nebula mass M(nebula) $\simeq 4.6\ M_{\odot}$ and the somewhat stronger constraint of the "central" weighted mean value of the glitch healing parameter $Q \approx 0.72$ are also imposed on these models. It follows, therefore, that the matching density, $E_{\rm b} = 2.7 \times 10^{14}$ g cm^{-3}, adopted in the present study itself results from the last two constraints imposed on the models. The confirmation of these results requires evidence of the observation of the gravitationally redshifted electron-positron annihilation line in the energy range of about 0.414–0.418 MeV. The evidence for a line feature at about 0.40 MeV from the Crab pulsar (Leventhal et al. 1977) agrees quite well with this result.

Furthermore, the study can also explain some special features associated with the extraordinary gamma-ray burst of 5 March 1979.

Acknowledgements. The author acknowledges the Aryabhatta Research Institute of Observational Sciences (ARIES), Nainital for providing library and computer-centre facilities, and U. C. Dumka for his help in preparing the figures of this manuscript. He would like to thank the referee for valuable comments.

References

Alpar, M. A., Chau, H. F, Cheng, K. S., & Pines, D. 1993, ApJ, 409, 345
Alpar, M. A., Chau, H. F, Cheng, K. S., & Pines, D. 1996, ApJ, 459, 706
Arnett, W. D., & Bowers, R. L. 1977, ApJS, 33, 415
Baym, G., Pethick, C., & Sutherland, P. 1971, ApJ, 170, 299 (BPS)
Bejger, M., & Haensel, P. 2002, A&A, 396, 917
Chandrasekhar, S. 1935, MNRAS, 95, 207
Cottam, J., Paerels, F., & Mendez, M. 2002, Nature, 420, 51
Crawford, F., & Demiański, M. 2003, ApJ, 595, 1052
Datta, B., & Alpar, M. A. 1993, A&A, 275, 210
Dolan, J. F. 1992, ApJ, 384, 249
Douchin, F., & Haensel, P. 2001, A&A, 380, 151
Friedman, J. L., & Ipser, J. R. 1987, ApJ, 314, 594
Hartle, J. B. 1978, Phys. Rep., 46, 201
Higdon, J. M., & Lingenfelder, R. E. 1990, ARA&A, 28, 401
Kalogera, V., & Baym, G. 1996, ApJ, 470, L61
Leventhal, M., MacCallum, C. J., & Watts, A. C. 1977, Nature, 266, 696
Lindblom, L. 1984, ApJ, 278, 364
Lorenz, C. P., Ravenhall, D. G., & Pethick, C. J. 1993, Phys. Rev. Lett., 70, 379 (FPS)
Negi, P. S., & Durgapal, M. C. 2001, Grav. & Cosmol., 7, 37
Negi, P. S. 2004a, Mod. Phys. Lett. A, 19, 2941
Negi, P. S. 2004b, Int. J. Mod. Phys. D, 13, 157
Negele, J., & Vautherin, D. 1973, Nucl. Phys., A207, 298 (NV)
Oppenheimer, J. R., & Volkoff, G. M. 1939, Phys. Rev., 55, 374
Pines, D., Shaham, J., & Ruderman, M. 1974, in Physics of Dense Matter, ed. C. J. Hansen (Dordrecht: Reidel), IAU Symp., 53, 189
Rhoades, C. E. Jr., & Ruffini, R. 1974, Phys. Rev. Lett., 32, 324
Ruderman, M. 1976, ApJ, 203, 213
Shapiro, S. L., & Teukolsky, S. A. 1983, Black Holes, White Dwarfs, and Neutron Stars: The Physics of Compact Objects (New York: Wiley)
Ulmer, M. P., Matz, S. M., Grove, J. E., et al. 2001, ApJ, 551, 244
Weinberg, S. 1972, in Gravitation and Cosmology (New York: Wiley)
Zeldovich, Ya. B. 1962, Soviet Phys., JETP, 15, 1158